

# Contrasting the termination of moderate and extreme El Niño events in coupled general circulation models

Matthieu Lengaigne · Gabriel A. Vecchi

Received: 20 November 2008 / Accepted: 19 March 2009  
© Springer-Verlag 2009

**Abstract** As in the observed record, the termination of El Niño in the coupled IPCC-AR4 climate models involves meridional processes tied to the seasonal cycle. These meridional processes both precondition the termination of El Niño events in general and lead to a peculiar termination of extreme El Niño events (such as those of 1982–83 and 1997–98), in which the eastern equatorial Pacific warm sea surface temperature anomalies (SSTA) persist well into boreal spring/early-summer. The mechanisms controlling the peculiar termination of extreme El Niño events, which involves to the development of an equatorially centred intertropical convergence zone, are consistent across the four models that exhibit extreme El Niños and observational record, suggesting that this peculiar termination represents a general feature of extreme El Niños. Further, due to their unusual termination, extreme El Niños exhibit an apparent eastward propagation of their SSTA, which can strongly influence estimates of the apparent propagation of ENSO over multi-decadal periods. Interpreting these propagation changes as evidence of changes in the underlying dynamical feedbacks behind El Niño could therefore be misleading, given the strong influence of a single extreme event.

**Keywords** El Niño/Southern Oscillation (ENSO) · Extreme events · IPCC-AR4 climate models · Coupled ocean–atmosphere mechanisms · Validation

## 1 Introduction

The El Niño/Southern Oscillation (ENSO) phenomenon is a dominant mode of climate variability on interannual time scales, and impacts weather patterns across the globe. The physical processes behind ENSO that involve coupling between the ocean and atmosphere in the tropical Pacific have been studied intensively over the past decades (e.g., Neelin et al. 1998; Wang and Picaut 2004 for reviews). As El Niño impacts strongly vary between events, depending on the characteristics of the warming (e.g., McPhaden et al. 2006), it is essential to better understand the mechanisms controlling its evolution. Although the amplitude and spatial structure can vary considerably from one warm ENSO (El Niño) event to another, a robust feature of El Niño is the tendency to peak to in boreal winter (Rasmusson and Carpenter 1982; Harrison and Larkin 1998). Here we contrast the evolution of extreme and moderate El Niños, with particular focus on the timing of and physical processes behind their peak and termination.

Figure 1 illustrates the characteristics of El Niños that are the focus of this manuscript by showing the evolution of near-equatorial conditions for extreme (top panels) and moderate (bottom panels) El Niños over the ERA40 period (1957–2002). Moderate and extreme El Niños both exhibit (by definition) warm sea surface temperature anomalies (SSTAs) across the eastern equatorial Pacific (EPAC); these warm SSTAs result in an eastward displacement of the west Pacific warm-pool and are associated with

---

M. Lengaigne (✉)  
Institut de Recherche pour le Développement/Laboratoire  
d’Océanographie et de Climatologie,  
Experimentations et Approches Numériques,  
Couloir 45-55, 4ème étage, Case 100, 4 place Jussieu,  
75252 Paris Cedex 05, France  
e-mail: lengaign@lodyc.jussieu.fr;  
lengaign@locean-ipsl.upmc.fr

G. A. Vecchi  
NOAA/Geophysical Fluid Dynamics Laboratory,  
Princeton, NJ, USA

increased precipitation in the central Pacific and a rainfall deficit in the western equatorial Pacific. El Niños exhibit westerly (positive) wind stress anomalies in the western and central equatorial Pacific prior to the onset of warm EPAC SSTAs (Rasmusson and Carpenter 1982; Harrison and Larkin 1998; Vecchi and Harrison 2000).

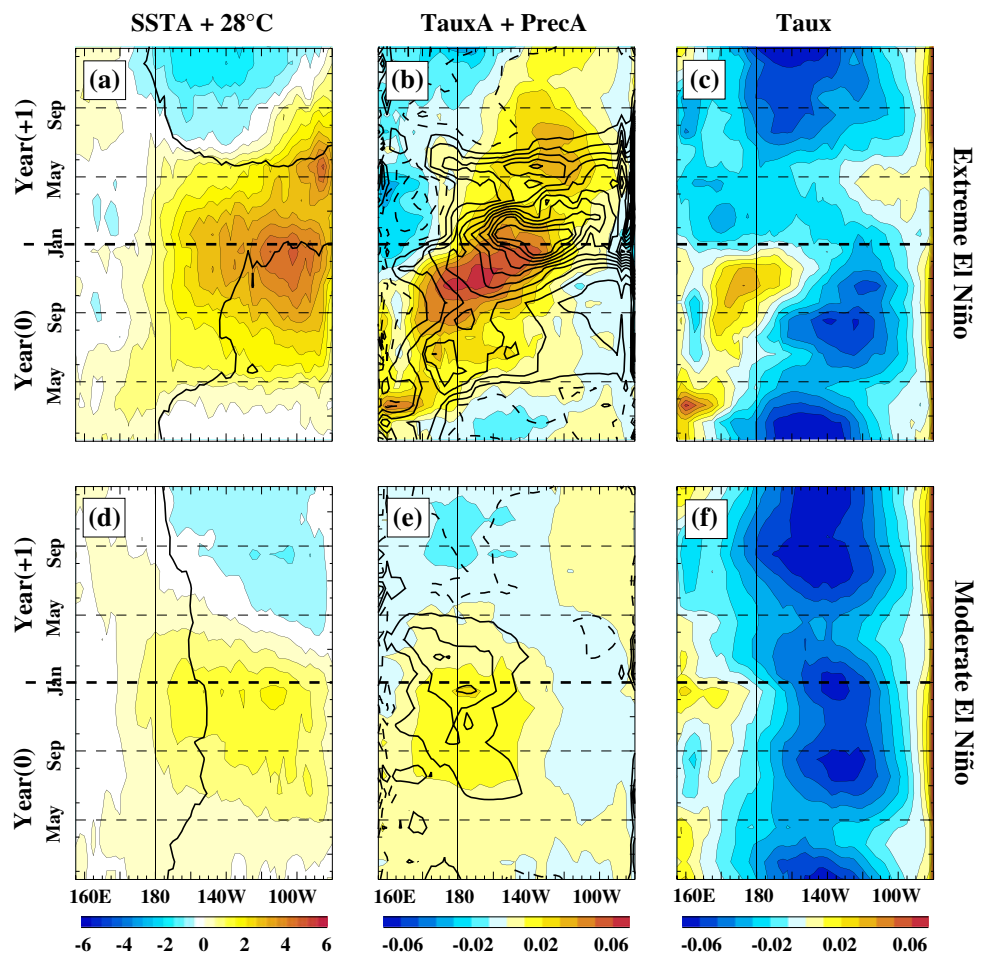
In moderate El Niños, the warmest surface waters (e.g. the 28°C isotherm in present climate) remain close to the Dateline throughout the event, with precipitation anomalies mainly in the western Pacific (Fig. 1d, e), SSTAs achieve their peak amplitude in December, the peak warm SST anomalies decay by March of Year(+1) and are centered between the Dateline and 140°W. The maximum westerly wind anomalies of moderate El Niños are confined to the western part of the basin, and decay at the end of Year(0). EPAC zonal winds remain easterly throughout El Niño, even exhibiting easterly anomalies east of 140°W for most of the event (Fig. 1f).

In contrast, the composite of two strongest El Niños have both the warmest surface waters and precipitation anomalies extending to the coast of South America in

winter and spring of Year(0)–Year(+1). East Pacific warm SSTAs exhibit two distinct peaks, one centered around 110°W in winter and a second peak evident along the coast of South America in boreal spring of Year(+1); these fluctuations in SSTA occur without much change in absolute SSTs, which remain relatively constant close to 29°C, so the SSTA variations reflect the absence/delay of the seasonal cycle. The eastern edge of the positive precipitation anomalies displays an apparent eastward propagation across the Pacific, reaching the eastern boundary by January of Year(+1); and the positive precipitation anomalies abruptly disappear in late-spring of Year(+1) (Fig. 1c). The maximum westerly wind anomalies also propagate across the basin to the coast of South America, resulting in a disappearance of the equatorial easterlies in the eastern part of the basin in boreal Spring of Year(+1). These characteristics are evident in each observed extreme El Niño, not just on average (Vecchi and Harrison 2006—VH06; Vecchi 2006—V06).

Both moderate and extreme El Niños show a decrease in their near-Dateline westerly wind anomalies at the end of

**Fig. 1** Time–longitude diagram for extreme El Niños (Year(0) = [1982, 1997]) of (a) equatorial SSTA (color), 28°C isotherm (thick line), (b) equatorial zonal wind stress anomaly (color), precipitation anomalies (lines) and (c) zonal wind stress (color). (d)–(f) Idem for moderate El Niños (Year(0) = [1963, 1965, 1969, 1972, 1976, 1977, 1979, 1987, 1991, 1994]). HadISST dataset (Rayner et al. 2003) is used for SST and ERA40 dataset is used for precipitation and wind stress



Year(+0) (Fig. 1b, d, Rasmusson and Carpenter 1982; Harrison 1987; Harrison and Larkin 1998). This decrease can be attributed to the southward shift of westerly anomalies in the western-central Pacific, away from the oceanic equatorial waveguide for both type of events. This southward shift has already been documented in observations (Harrison and Vecchi 1999; Vecchi and Harrison 2003) and is actually associated with the coupled response to seasonal changes in insolation (Vecchi and Harrison 2003; Spencer 2004; Lengaigne et al. 2007; V06; Xiao and Mechoso 2009). This reduction in westerly anomalies has been shown to drive the subsequent shoaling of the EPAC thermocline, preconditioning the termination of El Niño (Harrison and Vecchi 1999; Vecchi and Harrison 2003, Lengaigne et al. 2007). For the moderate events, the thermocline shoaling leads to a decrease in SST (Harrison and Vecchi 2001; Zelle et al. 2004), since equatorial easterlies are present throughout the event and upwell the cooling signal into the mixed-layer.

However, during extreme El Niño, the timing of the cooling in EPAC SSTs is not set (only preconditioned) by the thermocline shoaling. An analysis of the termination of the 1997–8 event illustrates the processes at play (VH06, V06). As the EPAC thermocline shoals, the local easterly winds disappear in spring (March to May), decoupling the cooling subsurface from the surface; only when the easterlies return in boreal late-spring/early-summer of Year(+1) does the return of upwelling leads to a sharp cooling of SSTs. The disappearance of the easterlies has been attributed to the development of an equatorial Inter-Tropical Convergence Zone (ITCZ), and the return of easterlies to the subsequent northward retreat of the equatorial ITCZ. It was suggested that this development and retreat of an equatorial ITCZ should be a general feature of extreme El Niños, and it was hypothesized that the ITCZ movement was tied to the seasonal March of insolation and the presence of warm SST anomalies of sufficient intensity to place the warmest waters on Equator (VH06, V06).

Thus, processes that are meridional in nature and tied to the seasonal cycle, have been suggested as fundamental to the termination of El Niños: the southward shift of near-Dateline westerly anomalies preconditions the termination of El Niños, and the development/retreat of an equatorial ITCZ prolongs and abruptly terminates extreme El Niños.

Here we show that the mechanisms controlling the peculiar termination of extreme events in 1997–98 and 1982–83 are active in a suite of state-of-the-art global climate models. These results confirm that this peculiar termination is likely to occur with observed extreme El Niños in general. Implications related to SSTA eastward/westward propagating signals associated with this peculiar termination are also discussed. We suggest that the prolonged EPAC warm anomalies lead to an apparent

eastward propagation of the termination of extreme events, which accounts for a large part of the eastward propagating SSTA signal associated with ENSO during the recent decades (1976–2000). The paper is structured as follows: “Extreme and moderate El Niño events in CGCMs” describes the IPCC database used, the differences between the termination of extreme and moderate El Niños in this database and the mechanisms explaining these differences. “Implications to apparent propagation of El Niño” discusses the implications related to SSTA eastward/westward propagating signals of the peculiar termination of extreme El Niños. Finally, “Summary and discussion” presents a summary and discussion of the results.

## 2 Extreme and moderate El Niño events in CGCMs

### 2.1 Multi-model database

The simulations analyzed in this paper are largely from models available via the Intergovernmental Panel on Climate Change Fourth Assessment Report (IPCC-AR4)/Coupled Model Intercomparison Project Three (CMIP3) database (Meehl et al. 2007), which offers references for the models at its website ([http://www-pcmdi.llnl.gov/ipcc/model\\_documentation/ipcc\\_model\\_documentation.php](http://www-pcmdi.llnl.gov/ipcc/model_documentation/ipcc_model_documentation.php)). The model list is given in Table 1, including their short names used in this paper. The first 24 models are taken from the IPCC-AR4/CMIP3 database managed by PCMDI. In addition to these 24 models, we make use of the Had-OPA model that is not part of the IPCC-AR4, but has been shown in several studies to display a realistic evolution and mechanisms in its onset and termination phase (Lengaigne et al. 2004, 2007). For all the models, the sea surface temperature (SST), the zonal wind stress ( $\tau_x$ ) and the precipitation (Pr) were analyzed. In addition, the depth of the 20°C when available has been used as a proxy of the thermocline depth in the equatorial Pacific.

In this study, we wish to focus on the internal variations of the coupled climate model systems, without introducing added complexity of changes in radiative forcing. We therefore study the set of experiments in which radiative forcing (and land use) is held at constant, pre-industrial values—this set of runs is referred to as the “Pre-Industrial Control” or `picntrl` experiments. However, the basic El Niño properties and the conclusions drawn from this study are not significantly altered if we explore the “Present-day Control” (`pdcntrl`) or the “Climate of the 20th century” (`20c3m`) experiments. The 25 datasets are interpolated (2-D linear interpolation) onto a common 2.5° longitude by 2.5° latitude grid. Monthly anomalies are calculated by removing a mean climatological cycle, and a 5-month running mean is applied to the anomalies

**Table 1** The models considered in this study, their short names used throughout the paper and the length of the simulations (in years)

Data name	Short name	Simulation length	$\sigma$ (SSTA <sub>Niño34</sub> )	% of events peaking in fall-winter (%)	Number of extreme-moderate events (peaking in fall-winter)
<b>HadISST (observations)</b>	<b>HadISST</b>	<b>45</b>	<b>0.82</b>	<b>92</b>	<b>2–10 (2–9)</b>
IAP-FGOALS-g1.0	IAP	350	1.81	94	0–103 (0–97)
<b>HadAM3-OPA</b>	<b>HadOPA</b>	<b>190</b>	<b>1.67</b>	<b>98</b>	<b>28–18 (28–17)</b>
<b>CNRM-CM3</b>	<b>CNRM</b>	<b>500</b>	<b>1.45</b>	<b>98</b>	<b>17–138 (17–135)</b>
<b>ECHAM5/MPI-OM</b>	<b>MPI</b>	<b>505</b>	<b>1.22</b>	<b>67</b>	<b>6–104 (6–68)</b>
MIUB-ECHO-G	MIUB	340	1.19	93	2–136 (2–127)
<b>GFDL-CM2.1</b>	<b>GFDL-1</b>	<b>500</b>	<b>1.15</b>	<b>66</b>	<b>14–88 (14–52)</b>
BCCR-BCM2.0	BCCR	250	0.90	71	0–69 (0–49)
GFDL-CM2.0	GFDL-0	500	0.87	65	0–139 (0–90)
IPSL-CM4	IPSL	500	0.86	65	0–159 (0–103)
UKMO-HadCM3	HADCM3	340	0.84	79	2–82 (2–64)
INM-CM3.0	INMCM	330	0.85	38	0–80 (0–30)
CSIRO-Mk3.0	CSIRO-0	380	0.82	58	0–112 (0–65)
NCAR-PCM1	PCM1	350	0.81	58	0–97 (0–56)
CSIRO-Mk3.5	CSIRO-5	130	0.77	52	0–29 (0–15)
INGV-ECHAM4	INGV	100	0.71	65	0–17 (0–11)
NCAR-CCSM3	CCSM3	130	0.75	68	0–47 (0–32)
MRI-CGM2.3.2	MRI	350	0.70	73	0–100 (0–73)
GISS-EH	GISS-EH	400	0.65	52	0–101 (0–53)
UKMO-HadGEM1	HADGEM1	240	0.63	61	0–64 (0–39)
MIROC3.2 (medres)	MIROC-MR	500	0.47	78	0–89 (0–69)
CCCMA-CGCM3.1(T47)	CCCMA-T47	500	0.42	74	0–128 (0–95)
CCCMA-CGCM3.1(T63)	CCCMA-T63	250	0.42	66	0–88 (0–58)
MIROC3.2 (hires)	MIROC-HR	100	0.32	61	0–23 (0–14)
GISS-ER	GISS-ER	500	0.17	53	0–115 (0–61)
GISS-AOM	GISS-AOM	250	0.15	45	0–65 (0–29)

The Niño34 SSTA standard deviation values (in °C), percentage of events peaking in the fall-winter seasons and the number of extreme and moderate El Niños are also added. The rows in bold are those models used in the analysis of El Niño characteristics

in order to focus on interannual variations in tropical climate conditions.

## 2.2 Diagnosing moderate and extreme El Niño events in CGCMs

El Niño amplitude in CGCMs is first diagnosed by calculating the SST anomalies (SSTA) averaged over the Niño3.4 region (170°–120°W, 5°N–5°S), which is often used in observations to identify El Niños. The monthly standard deviation ( $\sigma$ ) of Niño3.4 SSTA is shown in Table 1 for each model, and highlighting the large spread in the simulated ENSO amplitude ranging from 0.15 for GISS-AOM to 1.81 for the IAP-FGOAL. The inter-model variability of  $\sigma$  largely recovers the relative amplitudes of ENSO variability across the models as reported in the more comprehensive studies of ENSO in this set of models (Leloup et al. 2008; Guilyardi 2006; van Oldenborgh et al. 2005).

To objectively identify and quantitatively describe the evolution of El Niños in this database, we use a criterion similar to the one introduced by Trenberth (1997): an El Niño is defined for each dataset as a period where the Niño3.4 time series exceed  $\sigma/2$  during at least six consecutive months (the events selected with this method is not very sensitive to slight modifications of the event duration criterion). As we aim to contrast the termination of extreme and moderate El Niños, we need an objective criterion to distinguish between these two types of events. As discussed in the introduction, a peculiar feature for extreme El Niños (e.g. 1982–83 and 1997–98) is the displacement of the warm-pool and associated convective activity from the central to the eastern part of the equatorial Pacific in winter at the height of the event. Figure 2 display a scatter plot of the maximum (minimum) EPAC precipitation anomalies vs. the corresponding EPAC SSTA for each El Niño (La Niña) event. As expected, the precipitations show a non-linear response to SSTA for very warm conditions over the

1957–2001 period. All La Niña events and most El Niños display a rather weak precipitation response to SSTA. This is only for the two strongest El Niños (1982–83 and 1997–98) that intense rainfall occurs in the EPAC. Whereas most of the models display a nearly linear relationship between precipitation and SST anomalies (INMCM, BCCR, CSIROs, CCMAs, ...), 4 models (MPI, GFDL-1, CNRM, HadOPA) reproduce a clear nonlinear relationship with their warmest El Niños associated with the onset of convective activity in the EPAC (other panels in Fig. 2). As for observations, these strong precipitations mainly occur in DJF or MAM (i.e. during the peak and termination phase). The SSTA threshold related to the onset of convection depends on the models (e.g. 4°C for MPI and 2.5°C for HadOPA). To use a common criteria for observations and all models, we thus define as extreme El Niños those in which atmospheric deep convection develops in the EPAC such that precipitation anomalies in the equatorial eastern Pacific (120–90°W, 0°) exceed a 4 mm/day precipitation anomaly threshold during the event. Using this method, the 1997–98 and 1982–83 events falls into this category whereas all the other events during the 1957–2001 period are identified as moderate events. Among the models, only six of them are able to simulate extreme El Niños (HadOPA, CNRM, MPI, GFDL-1, MIUB and HadCM3). As only two extreme events develop in the MIUB and HADCM3 models, we will focus in the following on the evolution of El Niños in the four remaining models. These models are among those that display the strongest Nino3.4 SST standard deviation and reproduce reasonably well the observed phase of the seasonal cycle. However, the IAP model that simulates the strongest ENSO variability do not simulate extreme El Niños—this may be in part due to the very strong equatorial Pacific cold SST bias exhibited by this model, which keeps the warmest SSTs off equator even under extreme El Niño SST anomalies.

In the following, we will restrict our analysis to the events that reach their maximum amplitude in boreal fall or winter (September–February). For each model, the percentage of events occurring in boreal fall and winter seasons are indicated in Table 1. Most of the models underestimate the percentage of El Niños peaking during these seasons compared to observations. However, some of the models are able to recover the seasonal tendency in their simulated El Niños (e.g., HadOPA, CNRM-CM3, IAP, MIUB, HADCM3). These models are characterized by a relatively strong ENSO variability. In contrast, other models (CSIRO-5, CSIRO-0, GISS-EH, HADGEM1) display no seasonal phase locking.

Figure 3 contrasts the evolution of extreme and moderate El Niños (as defined previously), showing equatorial SSTA time–longitude diagrams for extreme and moderate El Niño composites for observations and the four models

considered (HadOPA, CNRM, MPI, GFDL-1). First, as expected, the average amplitude of extreme events is two- to three-times larger than that of moderate one. With regards to the spatial location of the SSTA, extreme and moderate El Niño development phase (Year(0)) are relatively similar within each model, at the onset of El Niño in CNRM the maximum positive SSTA is located in the eastern part of the basin, MPI and GFDL1 and in the central part for HadOPA. As expected, SSTAs mature in fall-winter season for all models and events. Though the development and peak phases of El Niño have similar SSTA patterns for extreme and moderate events within each model (although not of the same amplitude), the SSTA structure clearly differs during their termination. For moderate events, SSTA anomalies start decaying in spring of Year(+1) in the EPAC with a shift into “La Niña-like” conditions around May–June. In contrast, extreme El Niños display persistent positive SSTA in the EPAC that last well into boreal spring, along with an abrupt decay of the SSTA in early-summer (May to July, depending on the models). This behavior is qualitatively similar to the observed termination of the extreme and moderate El Niños, as displayed in Fig. 1a, b.

### 2.3 Coupled mechanisms involved in the extreme and moderate El Niño termination

To explore the mechanisms at play in the termination of moderate and extreme El Niños in these models, Fig. 4 contrasts the evolution of the SST and thermocline depth anomalies in the EPAC, and the near dateline zonal wind stress anomalies for the two types of events. The termination of moderate El Niños in these models can be easily understood by analyzing the evolution of the EPAC thermocline depth (only available for three of the four models). For these events, positive thermocline depth anomalies reach their maximum amplitude in winter (December–January) and rapidly decay from then on (Fig. 5f–h). This reduction in the thermocline depth directly decreases the SST by changing the temperature of the water upwelled and mixed vertically into the oceanic mixed-layer. SSTs return to near-normal values around May (Fig. 4a–e).

The EPAC thermocline shoaling follows, and is likely driven by, the strong decrease of the positive near-Dateline equatorial zonal wind stress anomalies beginning November of Year(0) occurring in all models and El Niño types (Fig. 4i–m). In observations and models, this central equatorial Pacific wind forcing decrease in winter is controlled by a southward shift of near-date-line wind anomaly field for simulated El Niños from November of the Year(0) (Fig. 5). This southward shift of the wind acts to reduce the strength of the equatorial westerlies near the Dateline, which results in a shoaling of the EPAC thermocline

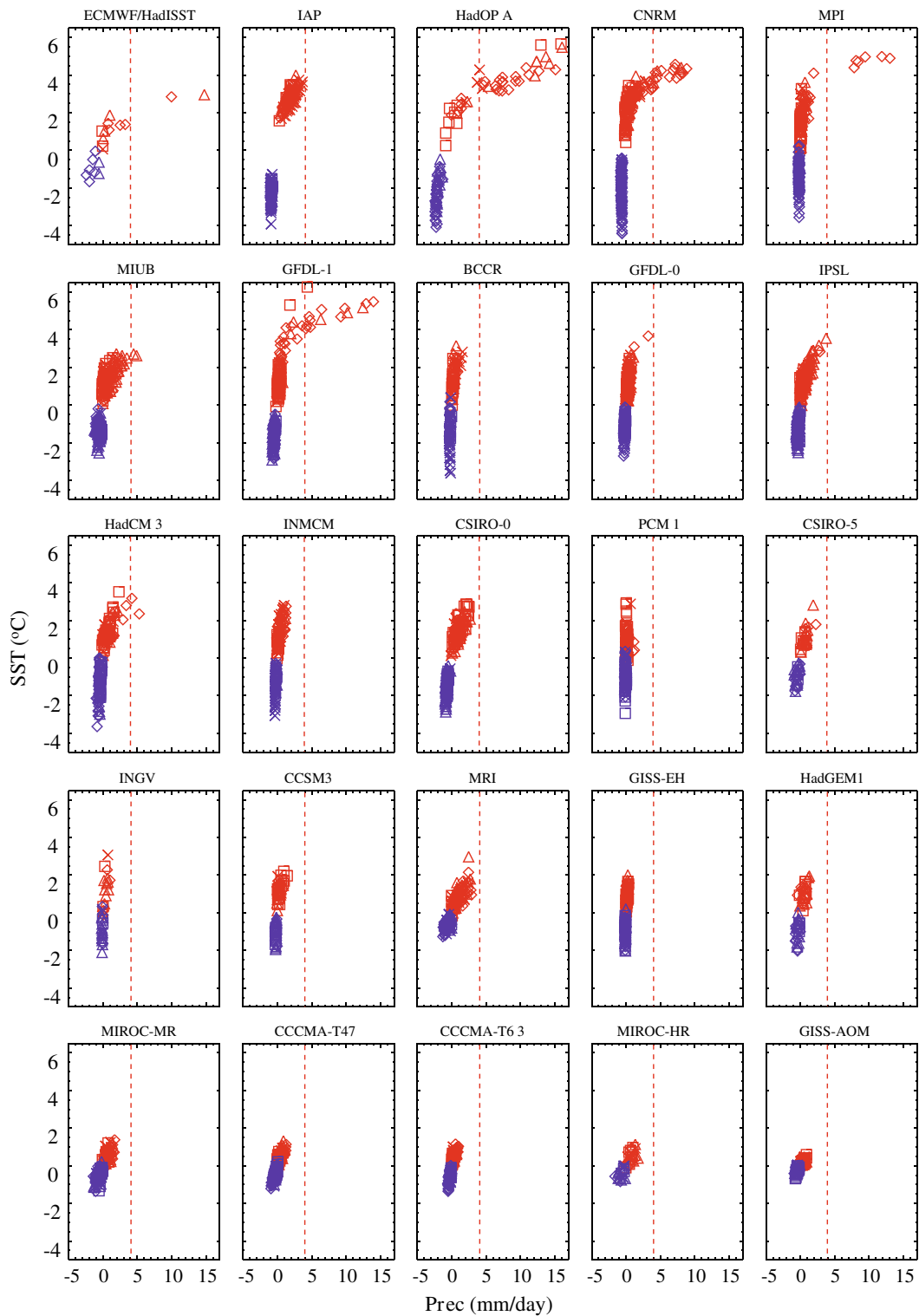


**Fig. 2** For the ERA40 analysis (*upper left panel*) and for each GCM listed in Table 1 (other panels, labeled with model name) a scatter plot of the maximum (minimum) eastern equatorial Pacific precipitation anomaly versus the corresponding eastern equatorial Pacific SSTA for each El Niño (La Niña) events. Different symbols are used for different seasons: *diamonds* corresponds to DJF, *triangles* to MAM, *squares* to JJA and *crosses* to SON. Warm colors indicate El

Niños and cool colors indicate La Niña events. Notice that in observations and in many models the strongest precipitations in the eastern Pacific mainly occurs in DJF or MAM, and that the observations and four of the models (CNRM, MPI, GFDL-1 and HADOPA) show nonlinear response of eastern equatorial Pacific precipitation for very warm SSTA

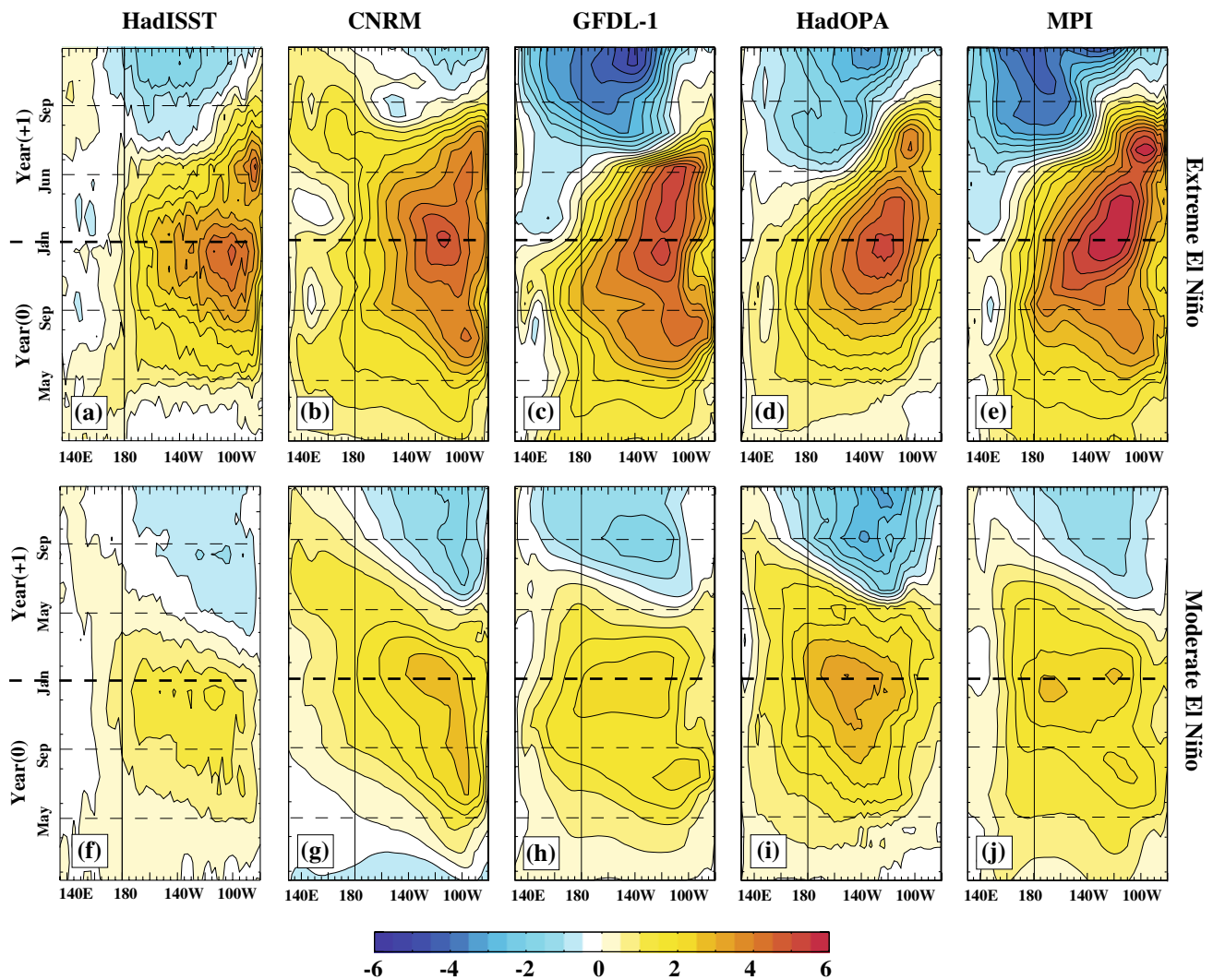


**Fig. 3** Time–longitude evolution of the equatorial Pacific SSTA for (a–e) extreme and (f–j) moderate El Niño composites for HadISST dataset and four climate models (CNRM, MPI, GFDL-1 and HADOPA)

through eastward propagating Kelvin pulses, and preconditions the termination of the El Niños.

The mechanisms controlling the termination of extreme El Niños exhibit further complexity, though some commonalities exist with those behind the termination of moderate events. As with the moderate events, in late autumn of extreme El Niños there is a decrease of the central equatorial Pacific zonal wind stress associated with a southward shift of the westerlies (Figs. 4i–m, 5); the central equatorial Pacific wind changes are followed by a rapid thermocline shoaling in the EPAC (Fig. 4f–h).

However, in contrast to moderate events, this southward wind shift and thermocline shoaling is not followed by a cooling in the EPAC (Fig. 4a–e). For these extreme events, the EPAC SSTAs remain significantly warmer than normal during the spring season while thermocline shoals. Then, in May–July, an abrupt and rapid SST cooling occurs, while

the thermocline depth has already been very close to its climatological conditions for some time. This prolonged warming is not readily understood in terms of the evolution of the EPAC thermocline in isolation. This peculiar period is characterized by a decoupling of the typically strong connection between SSTA and thermocline depth in the EPAC (Harrison and Vecchi 2001; Zelle et al. 2004; Zhang and McPhaden 2006, 2008).

To understand the period of shallow thermocline and warm SSTA at the end of extreme El Niños, we must explore local atmospheric changes. The very warm SST anomalies that develop for very strong El Niños (about +4°C) are associated with the development of strong precipitation anomalies in the eastern Pacific in winter (Fig. 6a–e). The establishment of a strong convective activity is accompanied by a relaxation of the trade winds in the EPAC (Fig. 6f–j). Thus, the weakening of EPAC

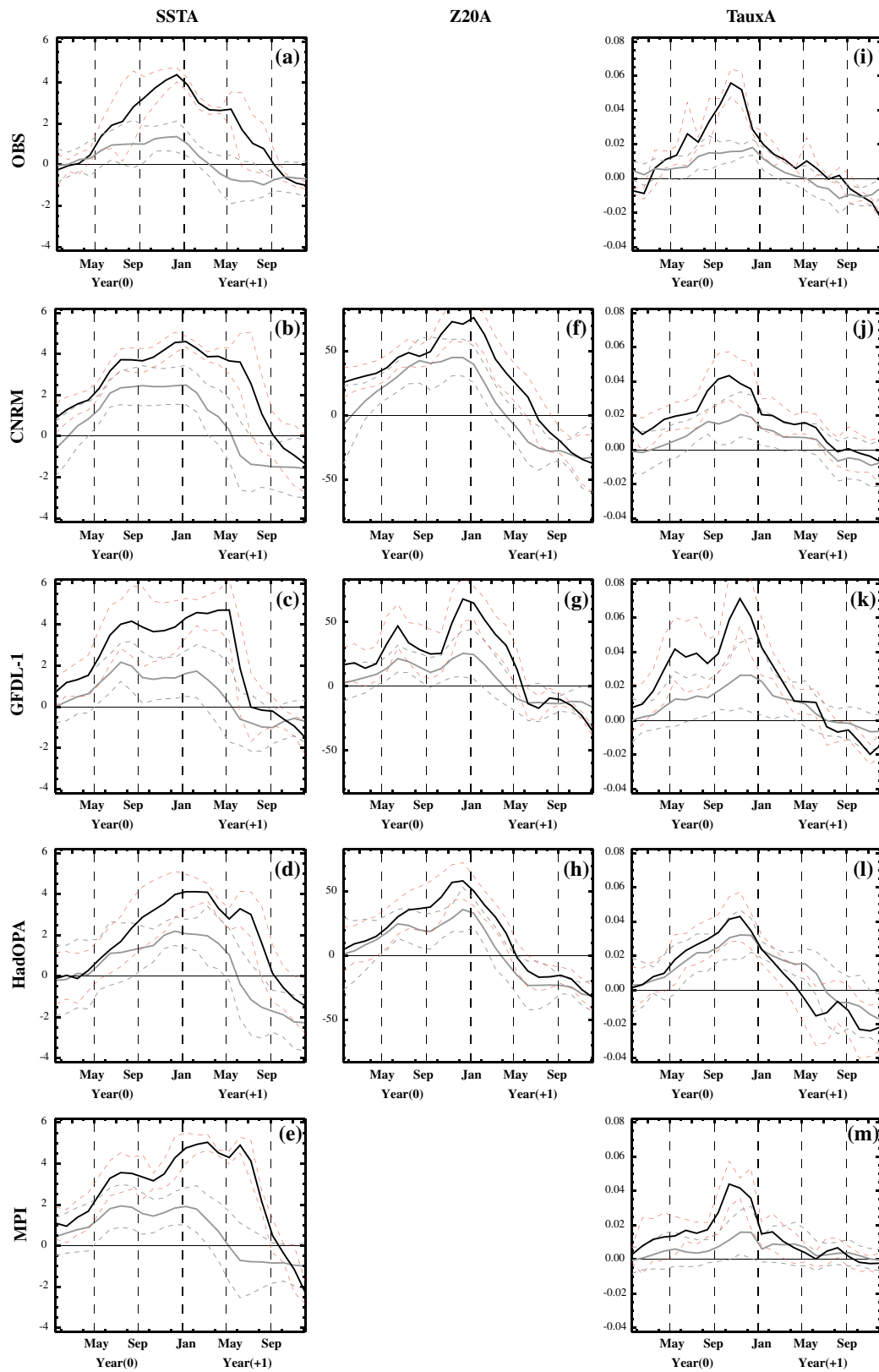
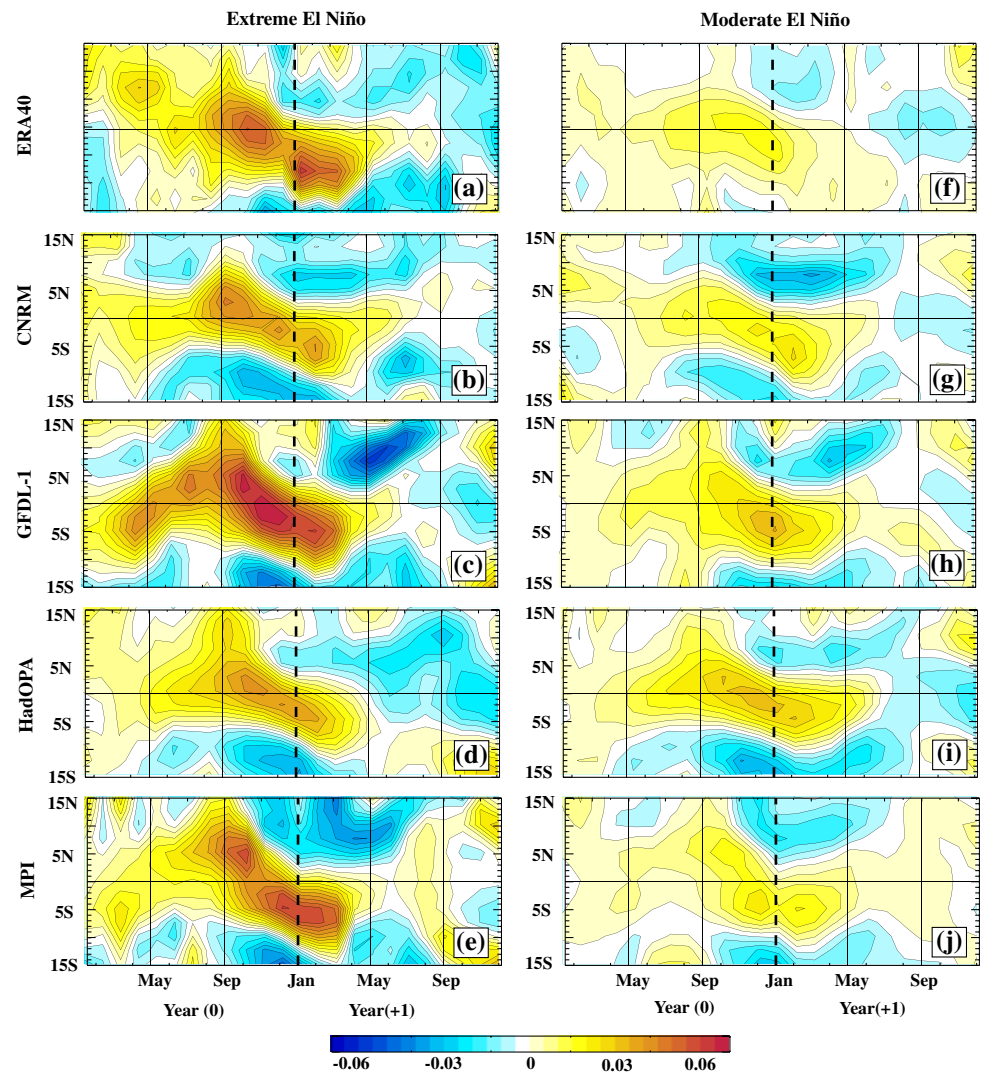


**Fig. 4** Time evolution at the equator for extreme (*solid black*) and moderate (*solid grey*) El Niño composites of **(a–e)** SSTA, **(f–h)** 20°C isotherm depth anomalies in the equatorial eastern Pacific (120°W–90°W) and **(i–m)** zonal wind stress in the central Pacific

(160°W–210°E) in observations (HadISST dataset and ERA40 Reanalysis) and four climate models (CNRM, GFDL-1, HADOPA and MPI). *Dashed lines* correspond to the composite mean  $\pm$  one standard deviation

**Fig. 5** Time–latitude evolution in the equatorial central Pacific (160°E–210°W) of zonal wind stress anomalies of (a–e) extreme and (f–j) moderate El Niño composites for ERA40 Reanalysis and four climate models (CNRM, GFDL-1, HadOPA and MPI)



easterlies leads to a reduction of wind-driven upwelling and mixing, and decouples the mixed-layer from the subsurface in the EPAC. Even as the thermocline shoaling beginning in December brings cold water closer to the surface, the relaxation of the local easterlies isolates the oceanic mixed-layer from these waters. This peculiar situation (shallow thermocline, warm SSTs, equatorial convection and reduced easterlies) lasts until late-spring/early-summer when the seasonal reinforcement of the easterlies rapidly cools the surface, ending the El Niño with an SSTA decay as strong as 2°C/month. During moderate events, on the other hand, the EPAC SSTA are not warm enough to allow the development of equatorial convection (Fig. 6a–e) in the eastern Pacific, keeping the zonal wind stress anomalies relatively weak in the eastern Pacific (Fig. 6f–j) and wind-driven mixing and upwelling is able to connect the mixed-layer with the subsurface as the thermocline shoals.

The development of this equatorial ITCZ during winter and spring for extreme El Niños in these models is actually the signature of a southward shift of the ITCZ from its usual location north of the equator to the equatorial region. Figure 7 contrasts the evolution of extreme and moderate El Niños in the eastern Pacific, showing time–latitude diagrams of SSTA, precipitation anomalies and warmest water edge for observations and the considered models. The SST threshold defining the meridional extent of the warm-pool differs among the models. In both moderate and extreme El Niños, the east Pacific SSTA is maximum on the Equator. However, the meridional location of the warmest east Pacific SST depends on the amplitude of the equatorial SSTA and the season. For moderate events, maximum SSTA reach 1–2°C in the EPAC. In this case, warmest SSTs remain located mainly north of the equator (5°N–15°N) with a tendency for all models to develop warm SST south of the equator during the spring season

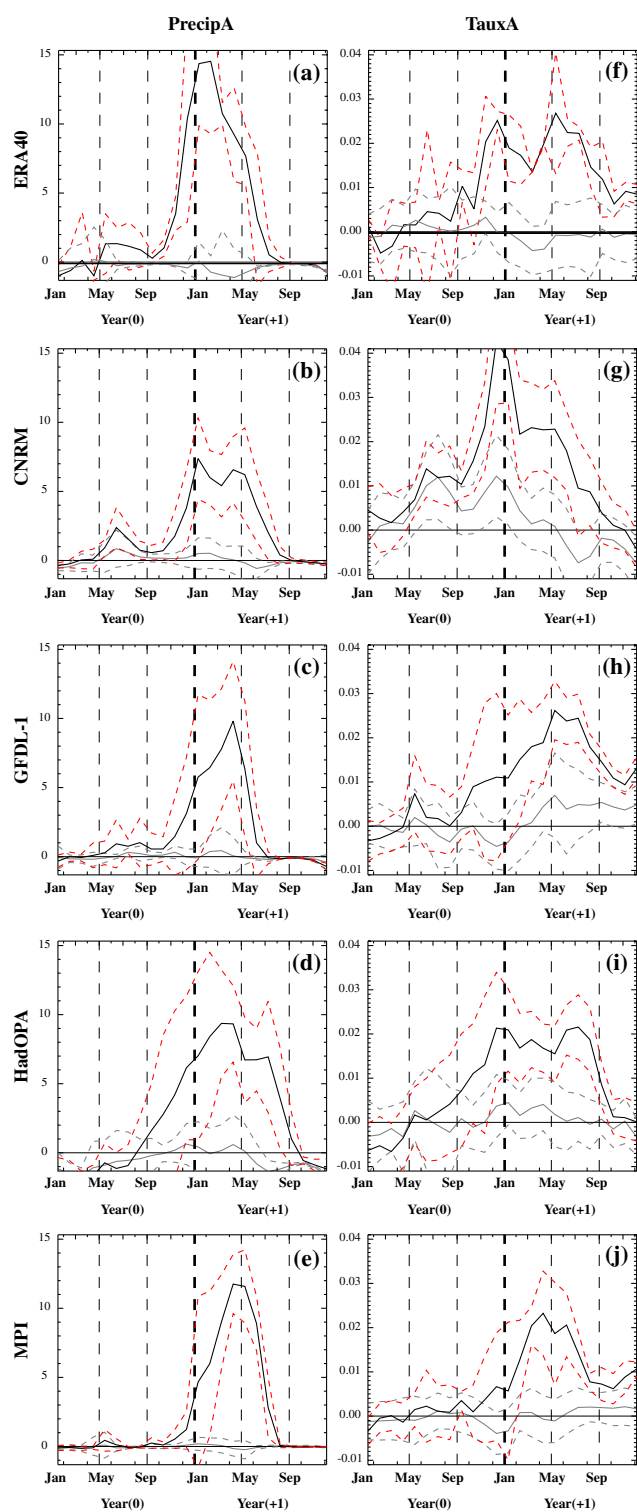


**Fig. 6** Time evolution at the equator for extreme (solid black) and moderate (solid grey) El Niño composites of (a–e) precipitation anomalies in the eastern Pacific ( $120^{\circ}\text{W}$ – $90^{\circ}\text{W}$ ) and (f–j) zonal wind stress anomalies in the eastern Pacific ( $140^{\circ}\text{W}$ – $90^{\circ}\text{W}$ ) in ERA40 Reanalysis and four climate models (CNRM, GFDL-1, HADOPA and MPI). Dashed lines correspond to the composite mean  $\pm$  one standard deviation

(the so-called double ITCZ problem). Thus, the warmest SST always remain out of the equatorial region during moderate El Niños as the equatorial SSTA are not strong enough to reverse the meridional SST climatological gradient. As a consequence, strong atmospheric convection and precipitation remain located out of the equatorial region.

For extreme El Niños, on the other hand, the equatorial SSTA in winter of about  $4^{\circ}\text{C}$  in the EPAC is strong enough to allow a meridional migration of the zone of maximum SST and convection close to the equator in January, leading to the relaxation of EPAC easterlies. Strong SSTA is maintained in the eastern Pacific until warmest SST and convective precipitations are shifted back north of the equator in relation with the seasonal March of insolation. As the equatorial easterlies strengthen the SSTA rapidly cools, terminating the El Niño in the eastern Pacific.

From this analysis, it appears that all models that are able to develop an equatorial ITCZ in the eastern Pacific during the mature phase of an El Niño simulate a prolonged eastern Pacific warming that last until May–July of Year(+1). This equatorial ITCZ develops as the strong EPAC SSTA leads to the warmest water displacement from the northern hemisphere to the Equator, and to the development of equatorial convection. The mechanisms controlling this peculiar termination of extreme El Niños in these models match those proposed in VH06 and V06 to explain the termination of the observed 1982–83 and 1997–98 El Niños. These results demonstrate that state-of-the-art climate models are able to simulate the subtlety of this termination and confirm that this peculiar termination character may be that expected to occur more generally in extreme El Niños.

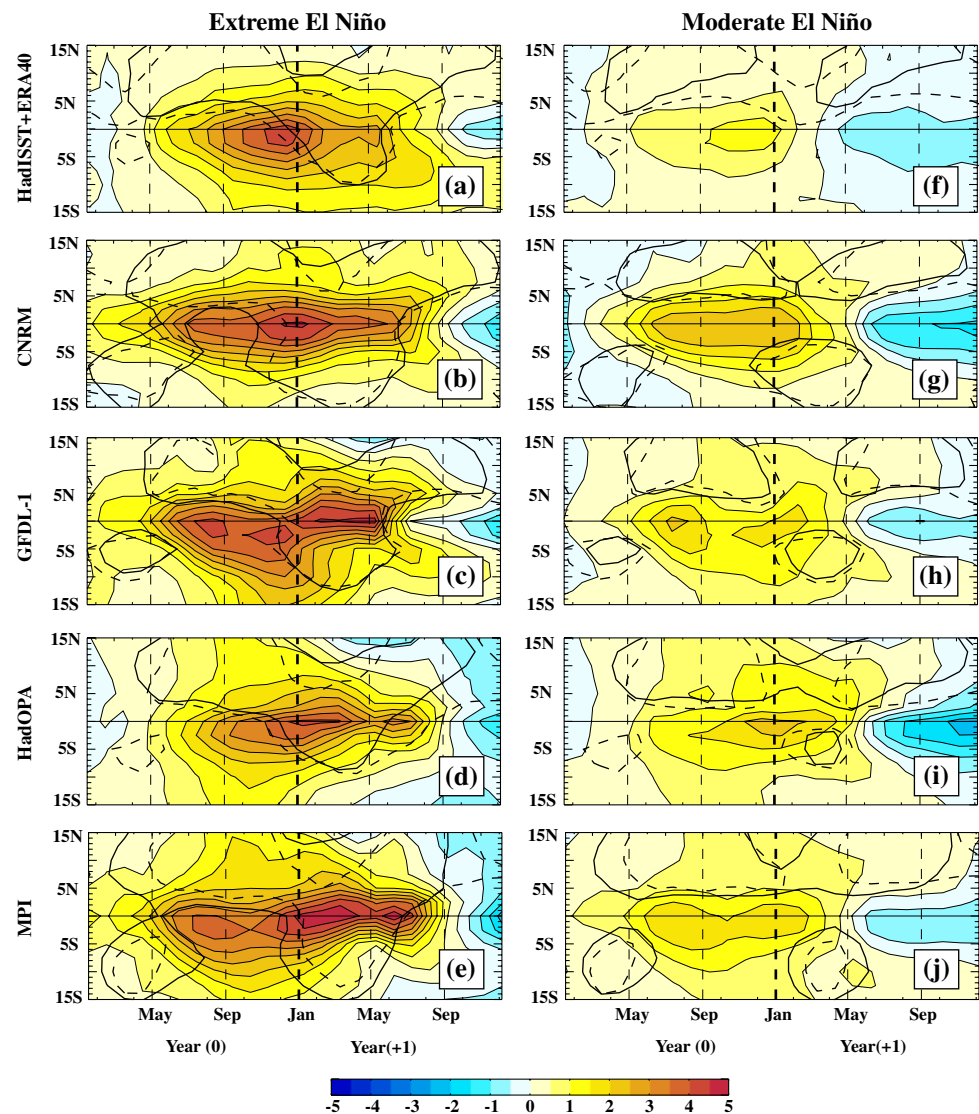
Interestingly, only models that display a larger than observed ENSO variability are able to simulated extreme events with intense precipitations in the eastern Pacific. This could be related to the cold bias in the equatorial cold tongue simulated in most of the CGCMs. EPAC SSTA therefore need to be stronger than in the observations to allow the onset of convection and the development of extreme El Niño events.

In the next section, we will discuss the implications of this peculiar termination of extreme El Niños in terms of SST propagating signals.

### 3 Implications to apparent propagation of El Niño

The zonal propagation characteristics of El Niños are of interest because they may contain information pertaining to the dominant mechanisms controlling ENSO (e.g., Trenberth and Stepaniak 2001; Federov and Philander

**Fig. 7** Time–latitude evolution in the equatorial eastern Pacific (120°W–90°W) of SSTA (color), 4 mm/day isoline precipitation anomaly (*solid line*) and warm-pool (*dashed line*) of (a–e) extreme and (f–j) moderate El Niño composites for observations (HadISST dataset and ERA40 Reanalysis) and four climate models (CNRM, GFDL-1, HadOPA and MPI). The warm-pool edge is defined as the 28°C for HadISST, 25.5°C for CNRM, 27.5°C for MPI and GFDL-1 and 29.5°C for HadOPA



2001; Burgers and van Oldenborgh 2003; Guilyardi et al. 2006). In this section, we explore the impact of the different termination behavior between extreme and moderate El Niños to their respective apparent propagation of SSTA, and discuss implications for the observed changes in propagation behavior and their interpretation.

As can be seen by contrasting the SSTA evolution in Fig. 1a, b, and contrasting the evolution in the top panels of Fig. 3 with that in the bottom panels, extreme El Niños exhibit a different apparent zonal propagation of their SSTA than do moderate events. Extreme El Niños tend to exhibit an eastward propagation of SSTA, while moderate El Niños exhibit a westward propagation. Comparing the time–longitude evolution of SSTA from moderate and extreme El Niños in Fig. 3, it can be seen that there is little difference in apparent propagation at the onset of the events, with the models and observations showing modest propagation (or in the case of the CNRM model a

substantial westward propagation) of SSTA for both extreme and moderate El Niños. However, the termination of the two kinds of events is characterized by fundamentally different propagation. Moderate events exhibit a rapid westward propagation of SSTA during their termination. Meanwhile, the termination of the observed extreme El Niños is characterized by an apparent eastward propagation of the SSTA cooling, associated with the persistence of EPAC warm SSTAs for 3–4 months after the near-Dateline cooling has begun (around January of Year(+1)).

We can formalize the descriptive analysis of propagation characteristics described in the previous paragraph by exploring an index commonly used to describe zonal propagation of SSTA. The propagation characteristics of ENSO can be estimated using the running lag-correlation of Niño3.4 to the Trans-Niño Index (TNI), which measures the east–west zonal gradient of SSTA by taking the difference between the normalized SSTA in the Niño

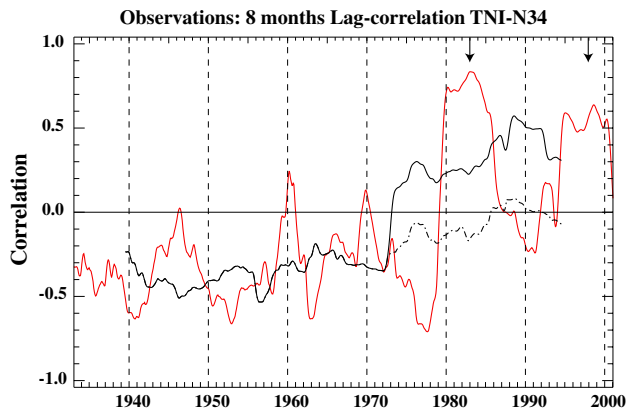


**Fig. 8** Eight-month lagged correlation of the Trans-Niño Index (TNI) with the normalized Niño34 SSTA over 1940–1995 period. *Red line* is for the 7-year running correlation, *solid black line* is for the 21-year running correlation and *dotted black line* is for the 21-year correlation with the 1983 and 1998 years removed. *Arrows* at the top of the figure highlight the 1982–3 and 1997–8 El Niños. Notice that the correlation is negative (indicating westward propagation) except for the influence of the two extreme El Niños

1 + 2 region in the east and the normalized SSTA in the Niño4 region in the central west Pacific. The lagged correlation of TNI and NIÑO3.4 (with TNI leading NIÑO3.4) indicates the dominant direction of propagation of ENSO anomalies, with negative (positive) values indicating westward (eastward) propagation (Trenberth and Stepaniak 2001). The solid black line in Fig. 8 shows the 20-year running correlation of 8-month lagged TNI and NIÑO3.4 ( $r_{8,20}(\text{TNI}, \text{NIÑO3.4})$ ), which exhibited a change in sign in the mid-1970s (Trenberth and Stepaniak 2001). This indicates that the dominant propagation of ENSO SST anomalies went from westward to eastward across the mid-1970s.

The strength of the mid-1970s shift in apparent ENSO propagation was strongly influenced by the two extreme events of 1982–83 and 1997–98. This can be seen by the red line in Fig. 8, which shows the 7-year running correlation of 8-month lagged TNI and NIÑO3.4. The two El Niños were the dominant source of eastward propagation. In fact, the termination phases of these extreme El Niños strongly influenced the character of the decadal  $r_{8,20}(\text{TNI}, \text{NIÑO3.4})$ . The dotted black line in Fig. 8 shows the result of computing  $r_{8,20}(\text{TNI}, \text{NIÑO3.4})$  without the termination phases of the 1982–83 and 1997–98. Without the termination of the extreme El Niños of 1982–83 and 1997–98, the mid-1970s shift in  $r_{8,20}(\text{TNI}, \text{NIÑO3.4})$  disappears and a smoother decadal reduction in the negative amplitude of  $r_{8,20}(\text{TNI}, \text{NIÑO3.4})$  is seen.

Figure 9 shows that three of the four climate models (HadOPA, MPI, GFDL1) exhibit a strong influence of the termination of extreme El Niños on the apparent propagation characteristics of ENSO (as computed using

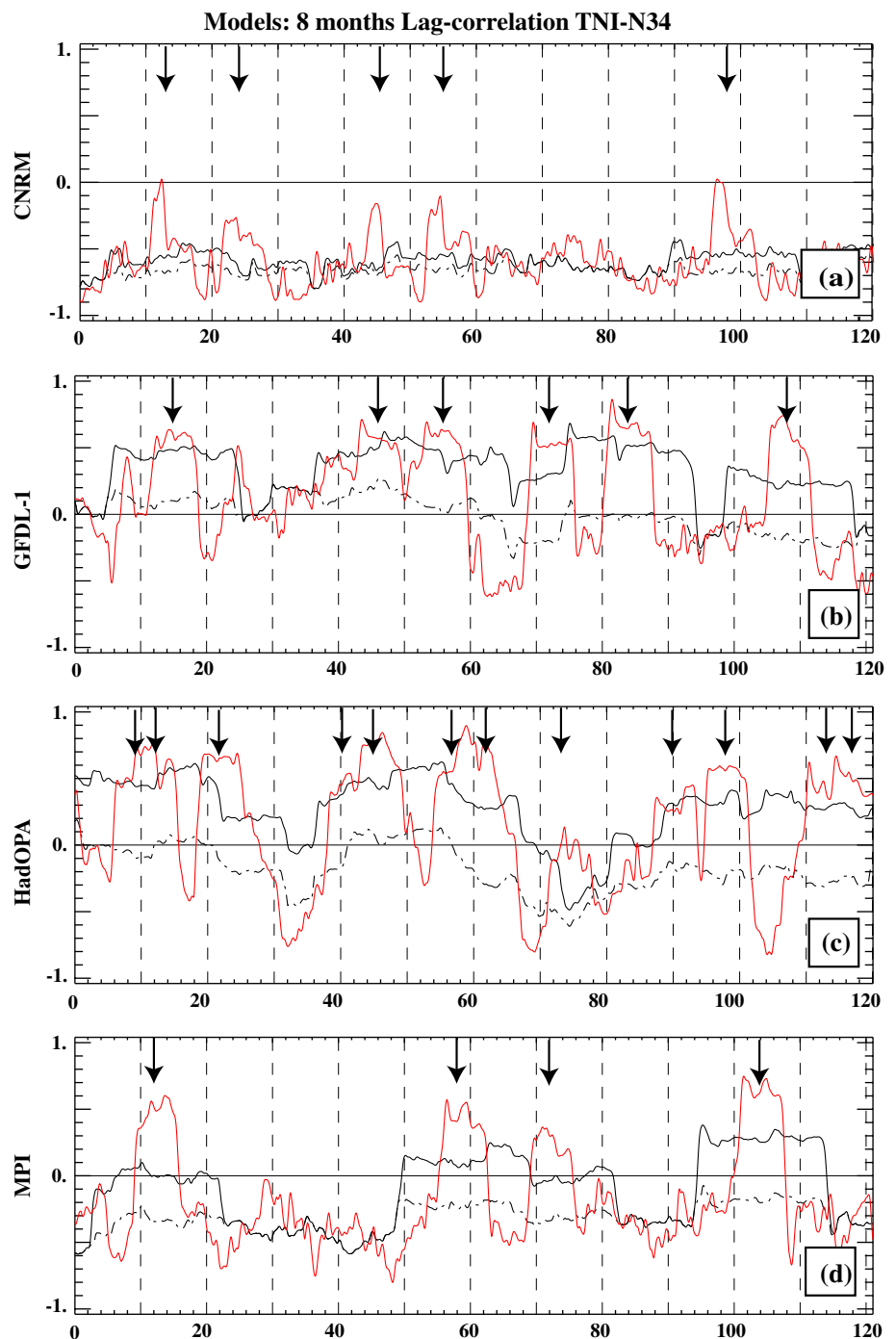
$r_{8,20}(\text{TNI}, \text{NIÑO3.4})$ ), similar to that seen since the mid-1950s (Fig. 8). As for observations, each of these models display decadal changes in apparent propagation of SSTA and eastward propagating periods are associated with extreme El Niños, and when these are removed (dotted lines), the overall. When removing Year(+1) of the simulated extreme El Niños from TNI SSTA correlation, the overall propagation tends to be either stationary or westward. For example, for the MPI model, 3 periods of positive correlations for positive lags are seen during the 150 years of correlation (Years 0–20, 45–80 and 95–115 in Fig. 9d). When we do not consider Year(+1) of the four extreme El Niños during that period (identified by the arrows) in the lag-correlations calculations, these correlations reverse sign and could be interpreted as an eastward propagating signal. This confirms that the termination of one extreme event can be responsible on its own for a positive correlation period of about 20 years. Similar results are found for HadOPA and GFDL models with the disappearance or weaker positive correlation for positive lags when removing the termination of simulated extreme El Niños.

Aspects of the propagation characteristics of ENSO are a therefore a consequence of the amplitude of the El Niños, and the peculiar termination of extreme El Niños. This analysis therefore suggest that the eastward SST propagating periods in models and observations deduced from the TNI-Niño34 lag-correlation can be to a large part attributed to the peculiar termination of few extreme El Niños. Since aspects of the amplitude of extreme El Niños are partly stochastically forced (e.g., Lengaigne et al. 2003, 2004; Vecchi et al. 2006), the influence of the termination of extreme El Niños may limit the usefulness of interpreting changes in  $r_{8,20}(\text{TNI}, \text{NIÑO3.4})$  as an indication of changing large-scale deterministic dynamical constraints on ENSO. Calculating these lag-correlations over moving windows of 20-years period could artificially give the impression of long-term periods in which eastward propagation was dominant, when only a small subset of the events actually exhibited a dominant eastward propagation to their SSTs.

#### 4 Summary and discussion

An assessment of global climate model simulations indicates that termination mechanisms for El Niño recently identified in observed data, involving meridional movements of atmospheric convections, are present in the climate models; this includes the processes that precondition the termination of El Niños in general, and the mechanisms leading to a peculiar termination of extreme El Niños (such as those of 1982–83 and 1997–98), in which the Eastern Equatorial Pacific (EPAC) warm anomalies persist well

**Fig. 9** Eight-month lagged correlation of the Trans-Niño Index (TNI) with the normalized Niño34 SSTA for (a) CNRM, (b) GFDL1, (c) HadOPA and (d) MPI models. Red line is for the 7-year running correlation, solid black line is for the 21-year running correlation and dotted black line is for the 21-year correlation with the Year(+1) of extreme El Niños removed. Arrows at the top of the figure highlight extreme El Niños. Notice that the correlation is positive during periods including extreme El Niños



into boreal spring/early-summer in association with the development of an equatorially centred ITCZ. The mechanisms controlling the peculiar termination of extreme El Niños are consistent across the four models that exhibit extreme El Niños and observational record, suggesting that they represent a general feature of extreme El Niños. Further, due to their unusual termination, extreme El Niños exhibit an apparent eastward propagation of their SST anomalies, which can strongly influence estimates of the apparent propagation of ENSO over multi-decadal periods;

the influence of extreme El Niños on apparent propagation complicates interpretation of the physical mechanisms behind observed propagation changes.

Although El Niños tend to be phase locked to the annual cycle and mature in amplitude in boreal winter (Trenberth 1997), the termination of El Niños have been shown to vary from one event to another. Commonly, El Niños terminate with EPAC SSTAs diminishing in winter so that SST in this area is near-normal by early-spring (Harrison and Larkin 1998). However, the termination of the two extreme

1982–83 to 1997–98 have been shown to terminate unusually with warm EPAC SSTAs exceeding 4°C at the event peak and lasting well into boreal spring with a sharp decrease of the SSTAs in late-spring–early-summer (McPhaden 1999; Takayabu et al. 1999). An accurate simulation of the observed diversity of El Niño termination is important as these differences can have significant different climate impact. This study has evaluated the ability of 25 different state-of-the-art coupled ocean–atmosphere GCMs to simulate the termination of both moderate and extreme El Niños.

We define extreme El Niños as the events where atmospheric deep convection develops in the eastern Pacific, as it was the case for the two extreme observed events. Most of the CGCMs are unable to simulate the diversity of observed events. In their simulated events, convective anomalies never extend into the eastern Pacific. Only four models, characterized by a higher than observed ENSO variability, are able to simulate both type of events (HadOPA, MPI, GFDL-1, CNRM-CM3). For these models, simulated extreme events display a termination close to what observed in 1983 and 1998 with a prolonged eastern Pacific warming and a late decrease of the SSTAs late-spring/early-summer of Year(+1). In contrast, simulated moderate events display a decay of SSTA anomalies in the eastern Pacific from late winter and a return to normal conditions in spring. This results confirms that the distinctive termination observed in 1983 and 1998 is that to be expected for extreme El Niños in general.

In addition, we assessed the mechanisms responsible for the termination of moderate and extreme El Niños in these four models. For moderate events, a late year southward shift of the near dateline zonal wind stress anomalies greatly decrease its equatorial component and drives an EPAC thermocline shallowing. This change in the thermocline depth directly decreases the SST with a return to near-normal EPAC SST in late spring. For extreme El Niños, the southward shift of the near dateline winds and the EPAC thermocline shallowing is also clear. However, the very warm SST anomalies that develop for very strong El Niños are associated with the establishment of a strong convective activity in the eastern Pacific accompanied by a relaxation of the trade winds in that region. Even if the thermocline shallowing in winter makes cold water available, the strong relaxation of the easterlies decouple the surface and the subsurface in the eastern equatorial Pacific because there is a reduced wind-forced upwelling. This situation lasts until late-spring/early-summer when the seasonal reinforcement of the easterlies rapidly cools the surface, ending the El Niño with a rapid SSTA decay in early-summer. Because of the strongly nonlinear relationship between SST, wind stress and precipitation that leads to the development of the equatorial ITCZ in extreme El

Niño events, there is no analogue at the end of La Niña events; this is another non-symmetrical feature of El Niño and La Niña events.

Extreme and moderate El Niños exhibit distinct equatorial SSTA zonal propagation characteristics. Because warm SSTA persists in the EPAC for extreme El Niños, while the central Pacific cools—partly through upwelling driven by strong cross-equatorial winds (e.g., Picaut et al. 2002)—extreme El Niños exhibit a strong eastward propagating SSTA signal at their end in both models and observations (Fig. 4). Meanwhile, moderate El Niños have strong EPAC easterly trade winds through their end-phase, so EPAC SSTA cools as the thermocline shoals—thus giving them a dominantly westward propagation of SSTA at their end. We have shown that a single extreme El Niño can influence estimates of apparent zonal SSTA propagation over 20 years (“Summary and discussion”), both in observations and the climate models. Using a commonly used estimate of propagation (lagged correlation of TNI and NIÑO3.4, e.g., Trenberth and Stepaniak 2001; Guilyardi 2006), an extreme El Niño can make it seem that the period was characterized by eastward propagation, though the signal is dominated by the end-phase of a single event. Thus, an accurate interpretation of apparent propagation of SSTA must account for the impact of the termination of extreme El Niños. Interpreting changes in the propagation of SST as evidence of changes in the underlying dynamical feedbacks behind El Niño (e.g., Guilyardi 2006; Guilyardi et al. 2008) could be misleading, given the strong influence of the end of a single event.

The establishment of equatorial convection in the eastern part of the basin is actually a manifestation of a southward shift of the Intertropical Convergence Zone from the north to the equator. This study therefore underlines the importance of meridional processes tied to the seasonal cycle in the termination of El Niños in CGCMs: the southward shift of near-Dateline westerly anomalies preconditions the termination of El Niños, and the development/retreat of an equatorial ITCZ prolongs and abruptly terminates extreme El Niños. The importance of the late year southward shift of the near-dateline zonal wind anomalies in reducing the central Pacific equatorial zonal wind anomalies and contributing to the El Niño termination has already been underlined in through observational analyses (Harrison and Vecchi 1999; Vecchi and Harrison 2003), forced model studies (Spencer 2004; VH06; V06) and coupled model experiments (Vecchi et al. 2004; Lengaigne et al. 2007; Xiao and Mechoso 2009). A series of model studies (Spencer 2004; V06; Lengaigne et al. 2007) underlined that the annual cycle of insolation accounts to a large part to the near-dateline southward shift of zonal winds. Another meridional process important in setting the timing in the extreme El Niño termination in the

ITCZ is the southward shift of the ITCZ to the equator in the eastern Pacific responsible for the prolonged warming along the western south-American coast. These results are consistent with recent work highlighting the importance of such a features in the peculiar termination of the 1997–98 event (VH06, V06).

**Acknowledgments** Authors are grateful to Michael McPhaden, Eric Guilyardi, Hilary Weller and an anonymous reviewer for helpful comments. We also acknowledge the Program for Climate Model Diagnosis and Intercomparison (PCMDI) and the IPCC Data Archive at Lawrence Livermore National Laboratory (U.S. D.O.E.) for making the IPCC-AR4 model data made available.

## References

- Burgers G, van Oldenborgh GJ (2003) On the impact of local feedbacks in the Central Pacific on the ENSO cycle. *J Clim* 16:2396–2407. doi:[10.1175/2766.1](https://doi.org/10.1175/2766.1)
- Federov AV, Philander SG (2001) A stability analysis of tropical ocean-atmosphere interactions: bridging measurements and theory for El Niño. *J Clim* 14:3086–3101. doi:[10.1175/1520-0442\(2001\)014<3086:ASAOTO>2.0.CO;2](https://doi.org/10.1175/1520-0442(2001)014<3086:ASAOTO>2.0.CO;2)
- Guilyardi E (2006) El Niño-mean state-seasonal cycle interactions in a multi-model ensemble. *Clim Dyn* 26:329–348. doi:[10.1007/s00382-005-0084-6](https://doi.org/10.1007/s00382-005-0084-6)
- Guilyardi E, Wittenberg A, Fedorov A, Collins M, Wang C, Capotondi A, van Oldenborgh GJ, Stockdale T (2008) Understanding El Niño in Ocean–Atmosphere General Circulation Models : progress and challenges. *Bull Am Met Soc* (in press)
- Harrison DE (1987) Monthly mean island surface winds in the central tropical Pacific and El Niño. *Mon Weather Rev* 115:3133–3145
- Harrison DE, Larkin NK (1998) Seasonal US temperature and precipitation anomalies associated with El Niño: historical results and comparison with 1997–1998. *Geophys Res Lett* 25:3959–3962. doi:[10.1029/1998GL900061](https://doi.org/10.1029/1998GL900061)
- Harrison DE, Vecchi GA (1999) On the termination of El Niño. *Geophys Res Lett* 26:1593–1596. doi:[10.1029/1999GL900316](https://doi.org/10.1029/1999GL900316)
- Harrison DE, Vecchi GA (2001) El Niño and La Niña—Equatorial Pacific thermocline depth and sea surface temperature anomalies, 1986–98. *Geophys Res Lett* 28:1051–1054. doi:[10.1029/1999GL011307](https://doi.org/10.1029/1999GL011307)
- Leloup J, Lengaigne M, Boulanger J-P (2008) Twentieth century ENSO characteristics in the IPCC database. *Clim Dyn* 30:277–291. doi:[10.1007/s00382-007-0284-3](https://doi.org/10.1007/s00382-007-0284-3)
- Lengaigne M, Boulanger J-P, Menkes C, Madec G, Delecluse P, Guilyardi E, Slingo JM (2003) The March 1997 Westerly wind event and the onset of the 1997/98 El Niño: understanding the atmospheric response. *J Clim* 16:3330–22243. doi:[10.1175/1520-0442\(2003\)016<3330:TMWWEA>2.0.CO;2](https://doi.org/10.1175/1520-0442(2003)016<3330:TMWWEA>2.0.CO;2)
- Lengaigne M, Guilyardi E, Boulanger J-P, Menkes C, Delecluse P, Inness P, Cole J, Slingo JM (2004) Triggering of El Niño by Westerly Wind Events in a coupled general circulation model. *Clim Dyn* 23:601–620. doi:[10.1007/s00382-004-0457-2](https://doi.org/10.1007/s00382-004-0457-2)
- Lengaigne M, Boulanger JP, Menkes C, Spencer H (2007) Influence of the seasonal cycle on the termination of El Nino events in a coupled general circulation model. *J Clim* 19:1850–1868. doi:[10.1175/JCLI3706.1](https://doi.org/10.1175/JCLI3706.1)
- McPhaden MJ (1999) Genesis and evolution of the 1997–98 El Niño. *Science* 283:950–954. doi:[10.1126/science.283.5404.950](https://doi.org/10.1126/science.283.5404.950)
- McPhaden MJ, Zebiak SE, Glantz MH (2006) ENSO as an integrating concept in earth science. *Science* 314:1740. doi:[10.1126/science.1132588](https://doi.org/10.1126/science.1132588)
- Meehl G, Covey C, Delworth T, Latif M, McAvaney B, Mitchell J, Stouffer R, Taylor K (2007) The WCRP CMIP3 multimodel dataset: a new era in climate change research. *Bull Am Met Soc* 1383–1394
- Neelin JD, Battisti DS, Hirst AC, Jin FF, Wakata Y, Yamagata T, Zebiak SE (1998) ENSO theory. *J Geophys Res* 103:14261–14290. doi:[10.1029/97JC03424](https://doi.org/10.1029/97JC03424)
- Picaut J, Hackert E, Busalacchi AJ, Murtugudde R, Lagerloef GSE (2002) Mechanisms of the 1997–1998 El Niño–La Niña, as inferred from space-based observations. *J Geophys Res* 107:3037. doi:[10.1029/2001JC000850](https://doi.org/10.1029/2001JC000850)
- Rasmusson EM, Carpenter TH (1982) Variations in tropical sea surface temperature and surface wind fields associated with the Southern Oscillation/El Niño. *Mon Weather Rev* 110:354–384. doi:[10.1175/1520-0493\(1982\)110<0354:VITSST>2.0.CO;2](https://doi.org/10.1175/1520-0493(1982)110<0354:VITSST>2.0.CO;2)
- Rayner NA, DE Parker, Horton EB, Folland CK, Alexander LV, Rowell DP, Kent EC, Kaplan A (2003) Global analyses of sea surface temperature, sea ice, and night marine air temperature since the late nineteenth century. *J Geophys Res* 108:4407. doi:[10.1029/2002JD002670](https://doi.org/10.1029/2002JD002670)
- Spencer H (2004) Role of the atmosphere in the seasonality of El Niño. *Geophys Res Lett* 31:24104. doi:[10.1029/2004GL021619](https://doi.org/10.1029/2004GL021619)
- Takayabu YN, Iguchi T, Kachi M, Shibata A, Kanzawa H (1999) Abrupt termination of the 1997–98 El Niño in response to a Madden-Julian oscillation. *Nature* 402:279–282. doi:[10.1038/46254](https://doi.org/10.1038/46254)
- Trenberth KE (1997) The definition of El Niño. *Bull Am Metab Soc* 78:2771–2777. doi:[10.1175/1520-0477\(1997\)078<2771:TDOENO>2.0.CO;2](https://doi.org/10.1175/1520-0477(1997)078<2771:TDOENO>2.0.CO;2)
- Trenberth KE, Stepaniak DP (2001) Indices of El Niño evolution. *J Clim* 14:1697–1701. doi:[10.1175/1520-0442\(2001\)014<1697:LIOENO>2.0.CO;2](https://doi.org/10.1175/1520-0442(2001)014<1697:LIOENO>2.0.CO;2)
- van Oldenborgh G, Philip S, Collins M (2005) El Niño in changing climate: a multi-model study. *Ocean Sci* 1:81–95
- Vecchi GA (2006) The termination of the 1997–98 El Niño. Part II: mechanisms of atmospheric change. *J Clim* 19:2647–2664. doi:[10.1175/JCLI3780.1](https://doi.org/10.1175/JCLI3780.1)
- Vecchi GA, Harrison DE (2000) Tropical pacific sea surface temperature anomalies, El Niño, and equatorial westerly wind events. *J Clim* 13:1814–1830. doi:[10.1175/1520-0442\(2000\)013<1814:TPSSTA>2.0.CO;2](https://doi.org/10.1175/1520-0442(2000)013<1814:TPSSTA>2.0.CO;2)
- Vecchi GA, Harrison DE (2003) On the termination of the 2002–2003 El Niño event. *Geophys Res Lett* 30:1964. doi:[10.1029/2003GL017564](https://doi.org/10.1029/2003GL017564)
- Vecchi GA, Harrison DE (2006) The termination of the 1997–98 El Niño. Part I: mechanisms of oceanic change. *J Clim* 19:2633–2646. doi:[10.1175/JCLI3776.1](https://doi.org/10.1175/JCLI3776.1)
- Vecchi GA, Rosati A, Harrison DE (2004) Setting the timing of El Niño termination. *Bull Am Met Soc* 85:1065–1066
- Vecchi GA, Wittenberg AT, Rosati A (2006) Reassessing the role of stochastic forcing in the 1997–8 El Niño. *Geophys Res Lett* 33:01706. doi:[10.1029/2005GL024738](https://doi.org/10.1029/2005GL024738)
- Wang C, Picaut J (2004) Understanding ENSO physics—A review (2004). In: Wang C, Xie SP, and Carton JA (eds) *Earth climate: the ocean–atmosphere interaction*. AGU Geophysical Monograph Series, pp 1–54
- Xiao H, Mechoso CR (2009) Seasonal cycle ENSO Interactions: validation of hypotheses. *J Atmos Sci* (in press)
- Zelle H, Appeldoorn G, Burgers G, van Oldenborgh GJ (2004) The relationship between sea surface temperature and thermocline depth in the Eastern Equatorial Pacific. *J Phys Oceanogr* 34:643–655. doi:[10.1175/2523.1](https://doi.org/10.1175/2523.1)
- Zhang X, McPhaden MJ (2006) Wind stress variations and interannual sea surface temperature anomalies in the Eastern Equatorial Pacific. *J Clim* 19:226–241. doi:[10.1175/JCLI3618.1](https://doi.org/10.1175/JCLI3618.1)
- Zhang X, McPhaden MJ (2008) Eastern equatorial Pacific forcing of ENSO sea surface temperature anomalies. *J Clim* 21:6070–6079